Biotechnol Lett
https://doi.org/10.1007/s10529-024-03525-9

ORIGINAL RESEARCH PAPER

Amyloidogenesis of SARS-CoV-2 delta plus and omicron variants receptor-binding domain (RBD): impact of SUMO fusion tag

Sadegh Zargan · Hasan Jalili · Bahareh Dabirmanesh · Saba Mesdaghinia · Khosro Khajeh

Received: 13 April 2024 / Revised: 16 July 2024 / Accepted: 12 August 2024

Abstract

Purpose The RBD of SARS-CoV-2 mediates viral entry into host cells by binding to the host receptor ACE2. SARS-CoV-2 infection is linked to various health issues resembling amyloid-related problems, persuading us to investigate the amyloidogenicity of the SARS-CoV-2 spike RBD.

Methods The FoldAmyloid program was used to assess the amyloidogenic propensities in the RBD of Delta Plus and RBD of the Omicron variant, with and without the SUMO tag. After the expression of RBDs, purification, and dialysis steps were performed, subsequently the ThT assay, FTIR, and TEM were employed to check the RBD ability to form fibrils.

Results The ThT assay, TEM, and FTIR revealed the ability of RBD to self-assemble into β-sheet-rich aggregates (48.4% β-sheet content). Additionally, the presence of the SUMO tag reduced the formation of RBD amyloid-like fibrils. The amyloidogenic potential of Omicron RBD was higher than Delta Plus, according to both in silico and experimental analyses.

Conclusions The SARS-CoV-2 RBD can assemble itself by forming aggregates containing amyloid-like fibrils and the presence of a SUMO tag can significantly decrease the formation of RBD amyloid-like fibrils. In silico analysis suggested that variation in the ThT fluorescence intensity of amyloid accumulations in the two SARS-CoV-2 strains arises from specific mutations in their RBD regions.

Keywords Amyloidogenic properties · Delta plus · Omicron · RBD · SARS-CoV-2

S. Zargan · H. Jalili (✉)
Department of Life Science Engineering, Faculty of New Sciences and Technologies, University of Tehran, Tehran, Iran
e-mail: hjalili@ut.ac.ir

B. Dabirmanesh · S. Mesdaghinia · K. Khajeh
Department of Biochemistry, Faculty of Biological Sciences, Tarbiat Modares University, Tehran, Iran

Introduction

The Coronavirus disease-2019 (COVID-19), caused by the severe acute respiratory syndrome Coronavirus 2 (SARS-CoV-2) (Harrison et al. 2020), belongs to the order *Nidovirales* (Gulyaeva and Gorbalenya 2021), which includes viruses with a single-stranded, positive-sense RNA with a large genome ranging in size from 26 to 32 kb (Gorbalenya et al. 2006, 2020). SARS-CoV-2 has a genome of ~ 30 kb. (Malone et al. 2022). This large genome is annotated to possess 14 open reading frames (ORFs) encoding 9890 amino acids, making 27 proteins (Gorbalenya et al. 2006; Wu et al. 2020). SARS-CoV-2 comprises four main structural proteins, including envelope, membrane, nucleocapsid, and spike proteins (Huang et al. 2020). The fragment of spike protein, from amino acid 319 to 541, is known as the receptor-binding domain

Published online: 25 August 2024

(RBD) (Shin et al. 2021), which plays a central role in the disease process by binding to the angiotensin-converting enzyme-2 (ACE2) receptor, allowing the virus to enter the host cell and initiate infection (Li et al. 2003).

According to the World Health Organization (WHO), 775,678,432 confirmed cases have been infected with COVID-19, resulting in 7,052,472 deaths (WHO Coronavirus (COVID-19) Dashboard, 2024). Alongside the mortality caused by COVID-19, the long-term effects of this disease and the enduring effects of vaccines are still under discussion and investigation (Byambasuren et al. 2023). In the meantime, there are reports of COVID-19 patients suffering from an increase in the level of Alzheimer's disease (AD) progression (Chen et al. 2022; Patel et al. 2022) as well as an elevation in the level of β-amyloid (Aβ) in the blood (Hsu et al. 2021), interacting directly with fibrin and fibrinogen to cause blood hypercoagulation (Grobbelaar et al. 2021) and diabetes, which is linked to islet amyloid polypeptide (IAPP) (Young et al. 2015). All of these reports are associated with amyloidotic fibrillar aggregates. One crucial question is which SARS-CoV-2 structural proteins can form amyloid, as this knowledge is vital for understanding the pathogenesis of the disease, including long COVID-19 (Leung et al. 2023).

Amyloid fibril formation has a connection with the increased content of β-structure in a protein structure, resulting in its fibrillar aggregation (Jimenez et al. 1999). Remarkably, the SARS-CoV-2 proteins comprise various amyloid-forming sequences (Milton 2023; Tayeb-Fligelman et al. 2023); among them, the spike protein contains RBD, with a secondary β-structure content of 34.1% (Brindha and Kuroda 2022; Nystrom and Hammarstrom 2022). RBD is a vaccine candidate and a target for drug development (Fitzgerald et al. 2021); however, the amyloidogenicity of RBD is still unclear, and the main related question is the possibility of the SARS-CoV-2 RBD amyloidogenic characteristics and its difference among various SARS-CoV-2 strains. Due to the rapid mutation of SARS-CoV-2, certain species presently do not exist, and only Omicron subvariants have become prevalent worldwide (Farahat et al. 2022; Parums 2023). The present research, for the first time, was conducted with a particular emphasis on Omicron and Delta Plus RBDs, aiming to investigate the potential of RBD in the formation of amyloid fibrils and to identify the impact of small ubiquitin-like modifier (SUMO) fusion Tag on this phenomenon. Intending to elucidate the underlying reasons for the variations in amyloid formation potential within the RBD across different strains of SARS-CoV-2, we compared the amyloidogenic potential of RBD among two significant variants of SARS-CoV-2 (Delta Plus and Omicron strains) using the FoldAmyloid algorithm (Garbuzynskiy et al. 2010), an in silico method of predicting amyloidogenic regions in a protein sequence. As fusion tags can provide control over the aggregation of an amyloidogenic protein (Kronqvist et al. 2022), the impact of the SUMO tag, which can enhance protein solubility due to its external hydrophilic surface and inner hydrophobic core (Butt et al. 2005), was examined on the Thioflavin T (ThT) fluorescence intensity of RBD amyloid-like fibrils formation. The findings will be presented based on the analysis of purified RBD of Delta Plus and RBD of Omicron variant with and without SUMO tag, isolated from *Escherichia coli* (*E. coli*) (Fig. 1) using ThT kinetics assay, Fourier-transform infrared spectroscopy (FTIR) and transmission electron microscopy (TEM).

Materials and methods

Materials

All the materials used in the present study were of analytical grade and purchased from Merck (Germany). *E. coli* T7 SHuffle cells were obtained from Novagen (USA).

In silico assessment of amyloidogenic potential of RBD

Two SARS-CoV-2 variants, including Delta Plus (B.1.617.2.1) and Omicron (B.1.1.529) with and without SUMO tag, were selected to compare the amyloidogenic potential of RBD in these strains and identify amyloidogenic regions in this domain. For this purpose, Protein Data Bank (https://www.rcsb.org/; accessed on 1 February 2021) was used for sequence determination of the SARS-CoV-2 spike RBDs (residues 319-541 aa). The FoldAmyloid program (http://bioinfo.protres.ru/fold-amyloid/) was also applied to evaluate the

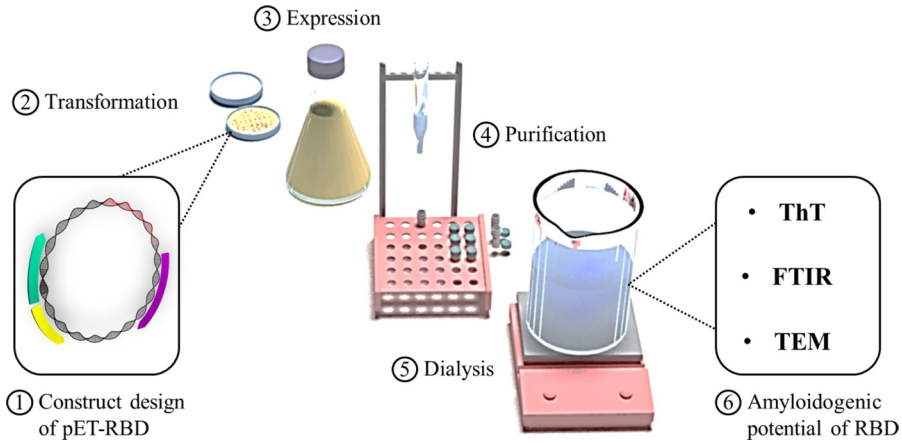

Fig. 1 Schematic workflow for evaluating the amyloidogenic potential of RBD

amyloid-forming ability of the RBDs (Nystrom and Hammarstrom 2022). This method predicts the amyloidogenic regions of the RBD by assessing the packing density and probability of backbone-backbone hydrogen bond formation. The amyloid-forming ability of the RBD was determined by dividing the percentage of the number of amino acid residues in the consensus amyloidogenic regions by the total number of amino acid residues on the protein. This calculation was conducted according to a protocol developed previously (Aksenova et al. 2022).

Plasmid constructs

The optimized Delta Plus (B.1.617.2.1) and Omicron (B.1.1.529) RBD genes were synthesized and cloned by Proteogenix (France) into *Nde*I and *Xho*I restriction sites of the expression vector pET-26b(+), which encodes 319–541 amino acid fragments of SARS-CoV-2 surface glycoprotein containing a 6×histidine tag at the *N*-terminus. To create the SUMO-RBD structure, we inserted the DNA encoding RBD (319-541 aa) of SARS-CoV-2 Omicron spike into the pET-21a(+) vector containing the SUMO fusion tag (Fig. 2). The resulting recombinant expression vectors were then transformed into T7 SHuffle competent

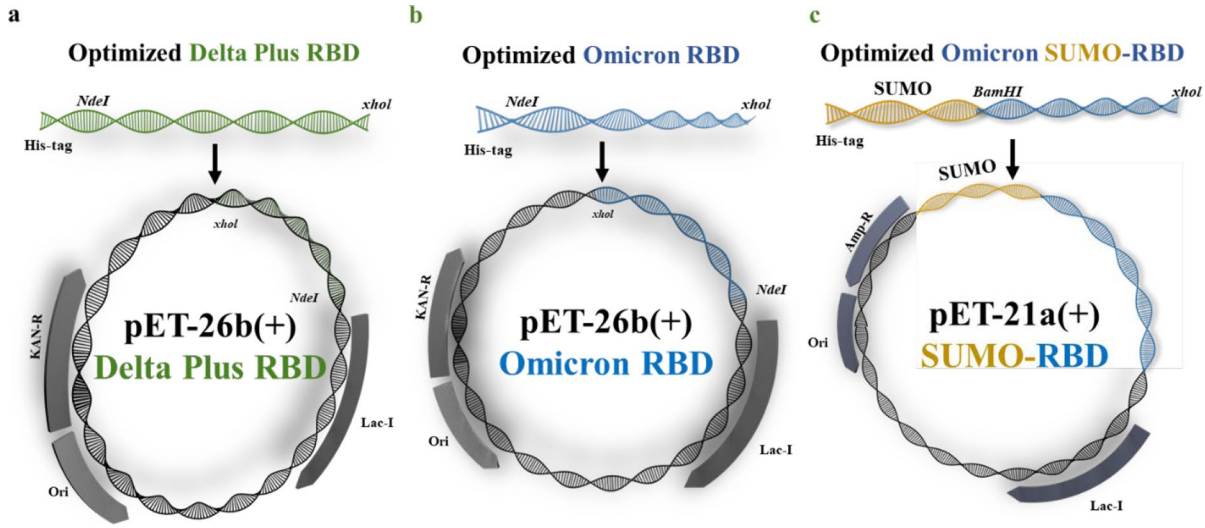

Fig. 2 The recombinant plasmid construct. **a** pET-26b(+) Delta Plus RBD, **b** pET-26b(+) Omicron RBD, and **c** pET-21a(+) Omicron SUMO-RBD

cells using the $CaCl_2$-mediated method (Dagert and Ehrlich 1979).

Protein expression and purification

T7 SHuffe cells transformed with the pET-26b (+) and pET-21a (+) vectors, containing the RBD and SUMO-RBD genes, respectively, were cultivated in a Luria–Bertani (LB) medium containing 100 µg/mL of antibiotic resistance markers at 30 °C overnight. Subsequently, 1 mL of the preculture medium was utilized to inoculate 100 mL of the LB medium. When the optical density at 600 nm (OD600) reached about 0.5, the protein expression was induced with 0.5 mM of isopropyl β-D-1-thiogalactopyranoside (IPTG). After 18 h of induction at 22 °C, the cells were harvested by centrifugation (4000×g, 20 min). Tris buffer (50 mM of Tris–HCL and 300 mM of NaCl; pH 7.5) was added to the cells and lysed by sonication on ice at 15 × 10 s, with a 50% duty cycle at 70% power. The resulting suspension was centrifuged at 12,000×g at 4°C for 20 min. The inclusion bodies were solubilized in a Tris–HCl buffer (pH 7.5) comprising 1 mM of dithiothreitol (DTT) and 8.0 M of urea. The unfolded protein was loaded on a Ni-Sepharose column (Amersham Biosciences, UK) that had been equilibrated with a 50-mM Tris buffer (pH 7.5) consisting of 10 mM of imidazole and 8.0 M of urea. Bound proteins were eluted with the same buffer used for column equilibration, containing 8 M of urea and 300 mM of imidazole. The protein purity was confirmed by SDS-PAGE according to the Laemmli method (Cleveland et al. 1977), and protein concentration was determined by the Bradford method (Bradford 1976).

ThT fluorescence

The benzothiazole dye ThT, a commonly employed method for diagnosing amyloid fibrils (Bolder et al. 2007), is known for its fluorescence enhancement when interacting with amyloid fibrils (Khurana et al. 2005). The ThT assay was carried out for SARS-CoV-2 Delta Plus and Omicron RBDs, which had a 6×histidine tag at the *N*-terminus. The assay was also conducted for the SARS-CoV-2 Omicron RBD with a SUMO fusion tag. The RBD stock solution, supplemented with 0.4 mg/mL of RBD and 0.65 mg/mL of SUMO-RBD, was prepared to equalize the molar concentration of RBDs in a 50 mM Tris–HCl buffer (pH 7.5) containing 8.0 M urea. Subsequently, this solution was loaded into a dialysis bag with a molecular weight cut-off of 10 kDa. The solution was then dialyzed against a 50-mM Tris–HCl buffer (pH 8.5) under stirring conditions at 4 °C for 30 h. At regular intervals, 60-µL samples of each RBD strain were collected before dialysis, and after 10 and 30 h of dialysis. These samples were then mixed with 440 µL of a 25-mM phosphate buffer (pH 6.0) containing 25 µM of ThT at 25 °C. The samples were measured for fluorescence in a range of between 450 and 550 nM at a 440-nM excitation wavelength, using a PerkinElmer Life Sciences LS-55 fluorimeter (Waltham, MA, USA) equipped with a thermostated cell compartment attached to a Haake F8 water bath (Karlsruhe, Germany), with a 2 × 10-mM path length cuvette.

Fourier-transform infrared (FTIR) spectroscopy

A sample of 4 mg/mL RBD in 8.0 M urea was dialyzed against a 50-mM Tris–HCl buffer (pH 8.5) with continuous stirring at 4 °C for 30 h. The sample underwent alternating centrifugation at 8050 g for 20 min at 25 °C. The resulting pellet was then resuspended in small amounts of D_2O, reaching a concentration of 12 mg/mL. The samples were placed on a CaF_2 window within a semi-permanent liquid cell, utilizing a 25 µM spacer. FTIR spectra were recorded within the range of 400 to 4000 cM^{-1} at 25 °C. Background subtraction was performed using a Jasco FTIR 4200 spectrophotometer (Tokyo, Japan) under a continuous flow of N_2. The amide I band (1600–1700 cM^{-1}) was isolated and baseline-corrected. The resulting spectrum was analyzed using Casa XPS software.

TEM

An EM 900A transmission electron microscope (Carl Zeiss NTS, Oberkochen, Germany) was used to achieve transmission electron micrographs. A small drop (~5 µL) of each RBD sample comprising RBD (0.4 mg/mL) in a 50-mM Tris–HCl buffer (pH 8.5), was deposited onto a copper 400 mesh grid covered with a perforated polymer film and a thin carbon layer. The images were visualized at a 40,000 × magnification.

Results

Amyloidogenic potential of SARS-CoV-2 RBD with and without tag

Amyloidogenicity is a significant factor affecting the interaction between hosts and pathogens (Ezzat et al. 2019). Therefore, the present study predicted the presence of amyloidogenic regions in Delta Plus (B.1.617.2.1) and Omicron (B.1.1.529) RBD amino acid sequences using the FoldAmyloid program. These amyloidogenic regions in polypeptide chains play a crucial role in forming and aggregating amyloids. Compared to SARS-CoV-2 wild type, Delta Plus (B.1.617.2.1) contained three RBD mutations (Starr et al. 2021). Predicting amyloidogenic regions in RBD from its sequence demonstrated the amyloidogenic potential of the Delta Plus strain as 22% (Fig. 3a), slightly higher than the Wuhan variant, which showed the potential of 18%. However, the Omicron variant with 15 mutations (Cao et al. 2022) indicated a 32% potential for amyloid formation compared to the Wuhan strain, mainly due to significant enhancement of the amyloidogenic potential in residues 369–381, 389–396, and 487–498 (Fig. 3b). In addition, the amyloid-forming ability of the Omicron RBD along with a SUMO tag was lower (22%) than the Omicron RBD without fusion (32%) (Fig. 3c).

Protein expression and purification

The most suitable conditions for protein expression were identified by investigating parameters such as temperature, induction time, and IPTG concentration. The effect of these factors on protein expression was qualitatively examined by SDS-PAGE (data not shown). The SARS-CoV-2 Delta plus and Omicron strain RBDs with a 6×histidine tag and SARS-CoV-2 Omicron RBD with a SUMO fusion tag expressed at high levels in T7 SHuffle cells with 0.5 mM of IPTG at 22 °C for 18 h. Subsequently, the unfolded RBD proteins were purified (Fig. 4).

ThT-positive aggregates of RBDs

Based on the ThT assay, which was accomplished using unfolded RBD with 8.0 M of urea, there were not any aggregates in the protein to bind ThT. Actually, no fluorescence emission at 485 nm was observed in the ThT fluorescence spectrum achieved. However, after the dialysis against Tris–HCl, the resulting samples were explored to bind the ThT dye and caused a significant fluorescence emission at 485 nM (Fig. 5).

The results of ThT assay also indicated that both the Delta Plus and Omicron strains of SARS-CoV-2 formed amyloid-like fibrils after 10-h dialysis and reached the highest levels of amyloid accumulation after 30 h. The fluorescence intensity of amyloid fibrils in the Omicron strain was slightly higher than that of the Delta Plus strain, which supports in silico prediction of this study, showing the presence of specific mutations in RBD regions of these strains.

The ThT assay was conducted for the RBD of the Omicron strain along with a SUMO fusion tag. The presence of the SUMO fusion tag effectively reduced the fluorescence intensity of amyloid accumulations in the Omicron SUMO-RBD (Fig. 6).

FTIR spectroscopy

FTIR is a well-established analytical technique for analyzing the secondary structure of proteins (Susi and Byler 1986). In the amide I region (1700−1600 cM^{-1}), various secondary structures lead to variations in the C=O stretching frequency, influenced by their distinct molecular shapes and hydrogen bonding patterns (Kong and Yu, 2007). Mathematical techniques, such as Fourier self-deconvolution (FSD), can resolve overlapping bands, enabling a quantitative estimation of protein secondary structure (Barth 2007).The Amide I region of the resultant FTIR spectrum of RBD amyloid-like fibrils revealed a peak at 1657 cM^{-1}, indicative of the α-helical secondary structure. The bands observed at 1621 and 1635 cM^{-1} can be attributed to inter- and intra-molecular β-sheet structures, respectively. Furthermore, the existence of β-turn structures is evidenced by the peaks at 1668 and 1690 cM^{-1} (Dong et al. 1992). After the analysis, it was determined that the secondary structure of the RBD amyloid-like fibrils consists of 48.4% β-sheet, 29.5% β-turn, and 5.6% α-helix (Fig. 7).

TEM results

Analyzing the morphological appearance of the RBD aggregates, formed after dialysis against Tris–HCl, by TEM displayed the presence of

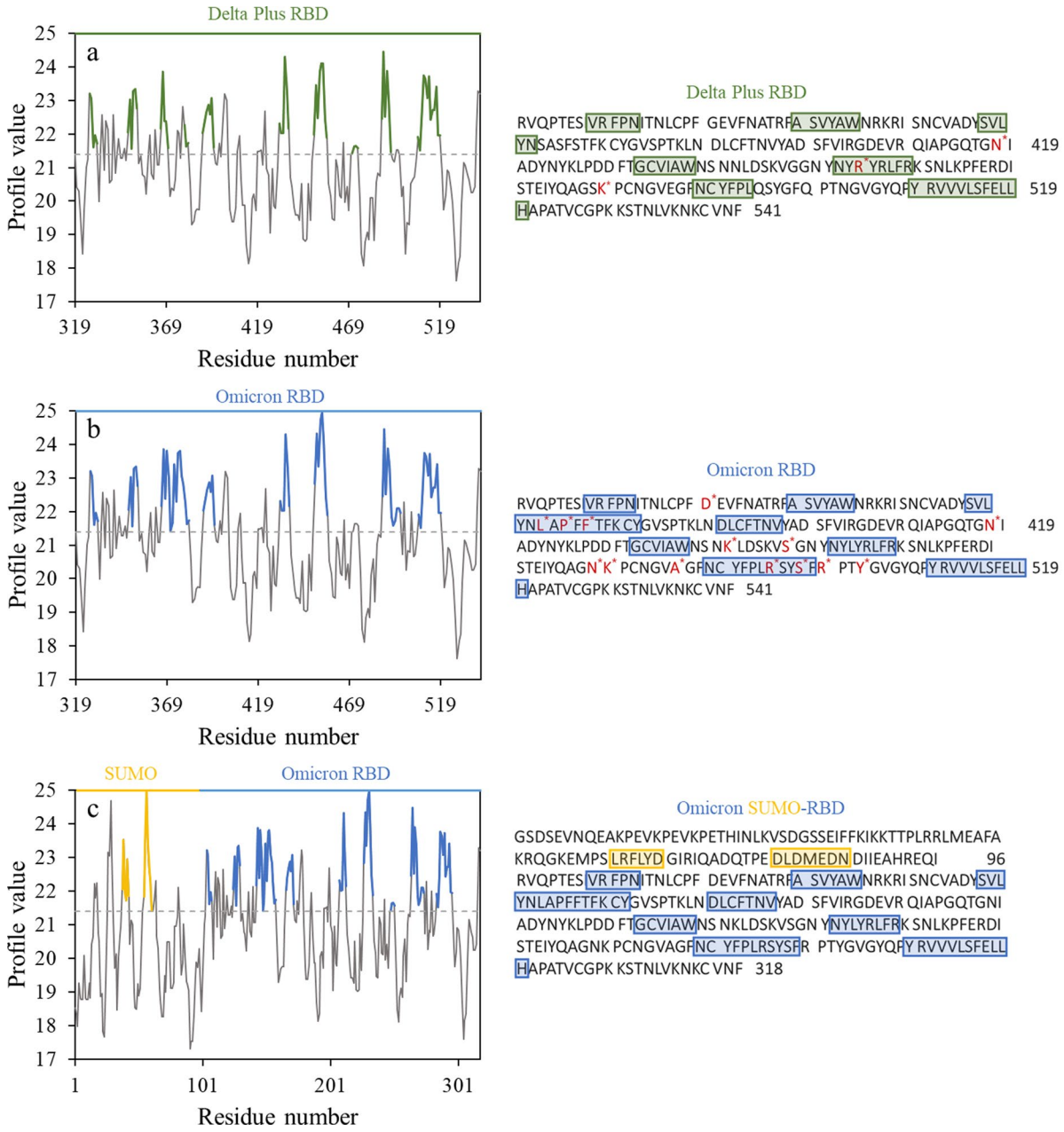

Fig. 3 The amyloidogenic regions of RBDs in two major SARS-CoV-2 variants, including **a** the Delta Plus [green sections] and **b** the Omicron strains [blue sections], predicted by FoldAmyloid. **c** The yellow and blue sections represent the SUMO and Omicron RBD regions in SUMO-RBD, respectively, Asterisks indicate the presence of amino acid mutations in the amyloid regions

elongated, uncomplicated fibrils (Fig. 8a and b). Fibrils often include two or more thinner filaments coiling around one another, resulting in a twisted ultrastructural appearance with regular periodicity. The fibril diameter was between 9 and 11 nM, a characteristic of amyloid fibrils. The morphology of amorphous aggregates was visualized by the rapid removal of urea through a dilution technique (Fig. 8c), and that of soluble proteins was examined by TEM (Fig. 8d).

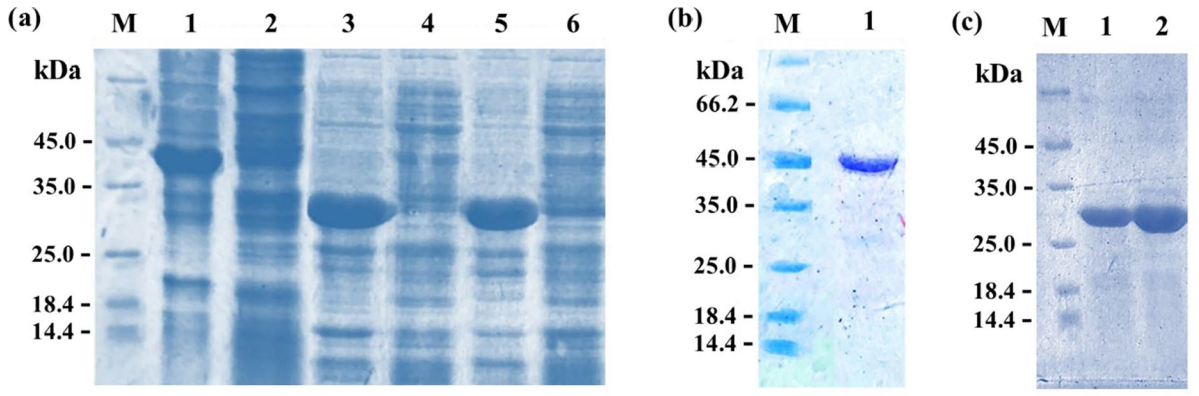

Fig. 4 SDS-PAGE showing the expression and purification of recombinant RBD and SUMO-RBD from *E. coli*. **a** *Lane M*: protein markers; *Lanes 1*, *3, and 5*: The Omicron SUMO-RBD (45 kDa), Omicron RBD (27 kDa), and Delta Plus RBD (27 kDa) inclusion bodies, respectively. *Lanes 2, 4, and 6*: soluble expression of total bacterial proteins of Omicron SUMO-RBD, Omicron RBD, and Delta Plus RBD, respectively. **b** *Lane M*: protein markers; *Lane 1*: purified SUMO-RBD. **c** *Lane M*: protein markers; *Lane 1*: purified Delta Plus RBD, and *Lane 2*: purified Omicron RBD

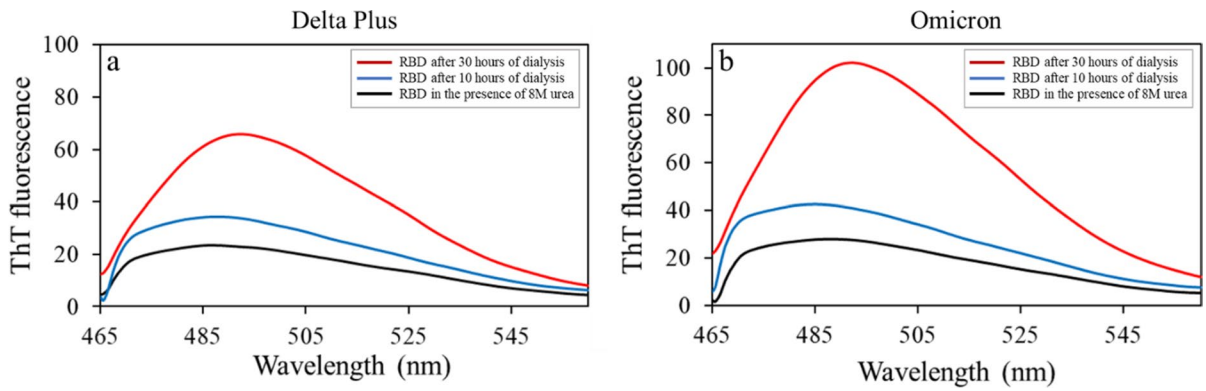

Fig. 5 ThT fluorescence spectra of Delta Plus (0.4 mg/mL) and Omicron (0.4 mg/mL) RBDs. RBD after 30 h of dialysis (red line), RBD after 10 h of dialysis (blue line), and RBD in the presence of 8 M urea (black line)

Discussion

RBD is a vaccine candidate against COVID-19 and a target for drug development (Yang et al. 2021). A large-scale Bacterially Expressed SARS-CoV-2 RBD could yield low-cost antigen for a subunit vaccine (Brindha et al. 2022; Liu et al. 2022), but it is crucial to note that its amyloidogenic properties may affect its effectiveness in vaccine development (Leung et al. 2023). Therefore, it is important to discover methods to decrease the aggregation of RBD amyloid-like fibrils. In a previous study, Sarr et al. demonstrated that fusion tags can reduce the aggregation of amyloid fibrils (Sarr et al. 2018). Solubility tags such as SUMO fusion tags can prevent the formation of inclusion bodies by stabilizing the proteins during expression (Butt et al. 2005). Therefore, the ThT assay was carried out for the RBD of the Omicron strain along with a SUMO fusion tag. The presence of the SUMO fusion tag effectively declined the ThT fluorescence intensity of amyloid accumulations in the RBD of the Omicron strain (Fig. 6), which is consistent with in silico predictions of the present study. This behavior can be attributed to the three-dimensional structure and solubility properties of the SUMO fusion tag, which have the potential to enhance the overall solubility of the fused protein (Butt et al. 2005). Furthermore, it is well-established that SUMO tags play

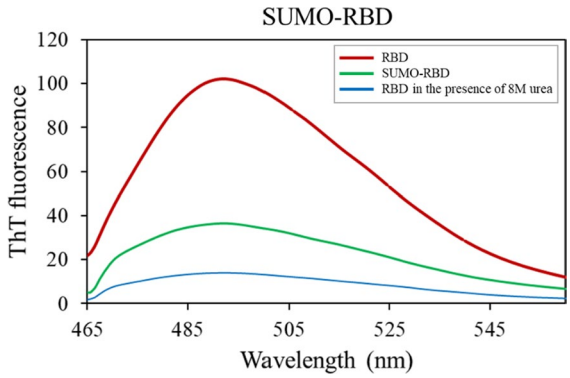

Fig. 6 ThT fluorescence spectra of Omicron RBD (0.4 mg/mL) and Omicron SUMO-RBD (0.65 mg/mL). Omicron RBD after 30 h of dialysis (red line), Omicron SUMO-RBD after 30 h of dialysis (green line), and RBD in the presence of 8 M urea (black line)

a crucial role in facilitating proper protein folding. By promoting correct folding, proteins are less susceptible to misfolding and aggregation (Marblestone et al. 2006). Moreover, the bulky nature of the SUMO fusion tag may create steric hindrance, thereby limiting the interaction between amyloidogenic regions in the RBD (Lee et al. 2008).

According to Nystrom and Hammarstrom's report, the full-length folded S-protein did not form amyloid fibrils. However, when the S protein was co-incubated with the protease neutrophil elastase (NE) in vitro for 24 h, it formed amyloid-like fibrils (Nystrom and Hammarstrom 2022). The key finding of this study is that the RBD was converted only into amyloid-like fibrils after the removal of urea (Fig. 9). Mutations can influence the severity of amyloid fibril formation, contingent upon various factors (Chiba et al. 2003; Greenbaum et al. 2005). For instance, amino acid mutations may destabilize the conformation of the protein, making it more likely to misfold and aggregate into amyloid fibrils (Marin-Argany et al. 2015). Furthermore, mutations can either accelerate or decelerate the rate of fibril formation, thereby influencing the overall severity of protein aggregation (Stefani and Dobson 2003). The ThT fluorescence intensity of amyloid accumulations differs among the strains of the SARS-CoV-2 virus can be attributed to specific mutations found in their RBD regions. The presence of amino acid mutations in the amyloid regions is indicated by an asterisk (*) in Fig. 3.

Conclusion

Overall, the study describes a cost-effective method for producing the SARS-CoV-2 RBD using *E. coli* T7 SHuffle cells, which offer low production costs, short generation times, and scalability. The RBD was successfully expressed with and without a SUMO tag and purified using a Ni Sepharose column. Biophysical techniques used in the present research found that the SARS-CoV-2 RBD can assemble itself by forming aggregates containing amyloid-like fibrils. Furthermore, in silico analysis of our study suggests that differences in the ThT fluorescence intensity of amyloid accumulations in Delta Plus and Omicron strains of the SARS-CoV-2 could be due to specific mutations in their RBD regions. The amyloidogenic

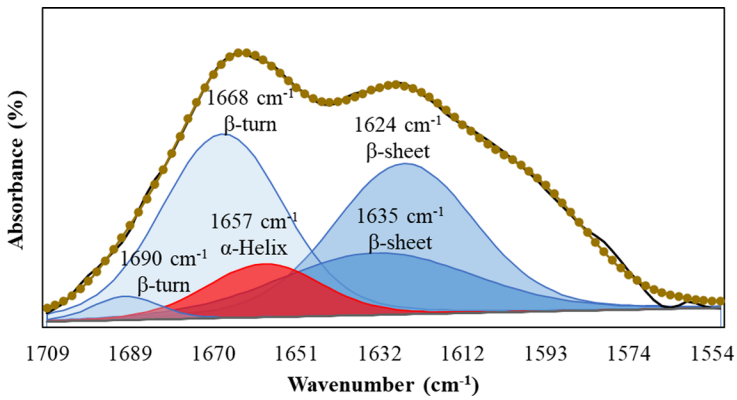

Secondary structure type	Curve fitting of FTIR spectrum
β-sheet	48.4%
β-turn	29.5%
α-helix	5.6%

Fig. 7 The FTIR spectrum (dotted line) and the peak deconvolution of the FTIR spectra for RBD amyloid-like fibrils, and summary of the secondary structure content obtained from FTIR spectrum analysis

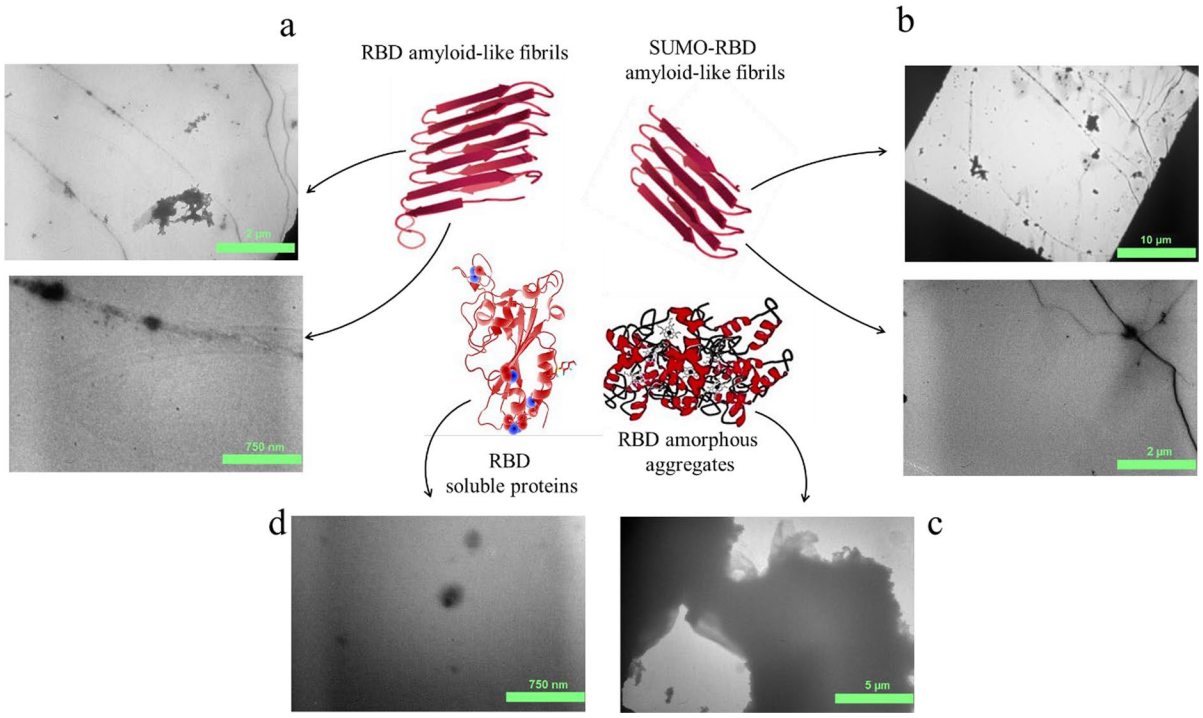

Fig. 8 TEM images showing β-sheet-rich aggregates with fibrillar, amyloid-like morphology formed from RBD after 30 h of dialysis (**a** and **b**), amorphous aggregates (**c**), and soluble RBD proteins (**d**) with the Protein Data Bank (PDB) code: 6M0J (available at https://www.rcsb.org/)

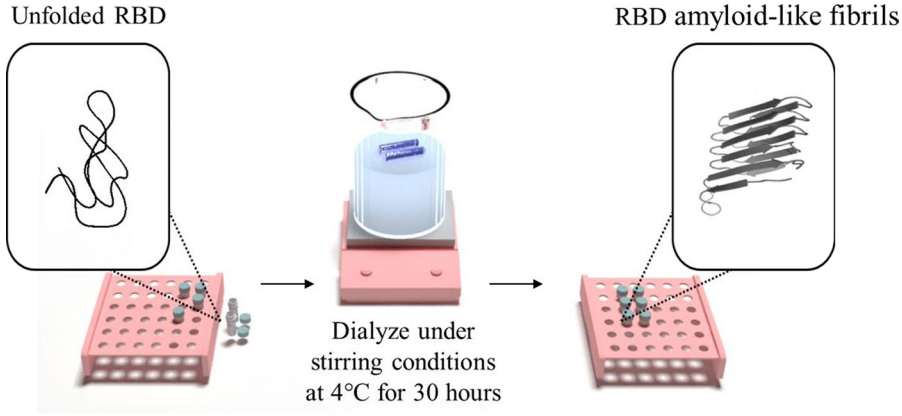

Fig. 9 Single-step formation of RBD amyloid-like fibrils

properties of the RBD are a significant challenge for vaccine development. The SARS-CoV-2 RBD forms amyloid-like fibrils only after the removal of urea. Strategies such as incorporating fusion tags are necessary to reduce amyloid formation, and the findings of this research reveal that the presence of a SUMO fusion tag can significantly decrease the formation of RBD amyloid-like fibrils. Hence, this question is raised: what other factors can reduce the formation of amyloids, and which strategies can be utilized in the vaccine industry? Our study has limitations, primarily due to the need for experimental validation under diverse physiological conditions to fully understand the impact and behavior of RBD amyloid-like fibrils in vivo. It would be better for future research to focus on in vivo studies to assess the effects of RBD-formed

amyloids on amyloid-related diseases and explore other inhibitors of amyloidogenesis.

Acknowledgements This work was supported by the University of Tehran and Tarbiat Modares University.

Author contributions SZ: carrying out experiments, analysis of data, writing the manuscript, visualization. HJ: development of the idea, supervision of the project, manuscript revision, technical support. BD: development of the idea, supervision of the project, validation, manuscript revise. SM: carrying out experiments, analysis of the data, manuscript revise. KK: development of the idea, supervision of the project, manuscript revise, technical support.

Funding The author(s) reported there is no funding associated with the work featured in this article.

Data availability Data will be made available upon request.

Declarations

Competing interests The authors have no relevant financial or non-financial interests to disclose.

References

Aksenova AY, Likhachev IV, Grishin SY, Galzitskaya OV (2022) The increased amyloidogenicity of spike RBD and pH-dependent binding to ACE2 may contribute to the transmissibility and pathogenic properties of SARS-CoV-2 omicron as suggested by in silico study. Int J Mol Sci 23:13502. https://doi.org/10.3390/ijms232113502

Barth A (2007) Infrared spectroscopy of proteins. Biochim Biophys Acta 1767:1073–1101. https://doi.org/10.1016/j.bbabio.2007.06.004

Bolder SG, Sagis LM, Venema P, van der Linden E (2007) Thioflavin T and birefringence assays to determine the conversion of proteins into fibrils. Langmuir 23:4144–4147. https://doi.org/10.1021/la063048k

Bradford MM (1976) A rapid and sensitive method for the quantitation of microgram quantities of protein utilizing the principle of protein-dye binding. Anal Biochem 72:248–254. https://doi.org/10.1016/0003-2697(76)90527-3

Brindha S, Kuroda Y (2022) A multi-disulfide receptor-binding domain (RBD) of the SARS-CoV-2 spike protein expressed in *E. coli* using a SEP-tag produces antisera interacting with the mammalian cell expressed spike (S1) protein. Int J Mol Sci 23:1703. https://doi.org/10.3390/ijms23031703

Brindha S, Yoshizue T, Wongnak R, Takemae H et al (2022) An *Escherichia coli* expressed multi-disulfide bonded SARS-CoV-2 RBD shows native-like biophysical properties and elicits neutralizing antisera in a mouse model. Int J Mol Sci 23:15744. https://doi.org/10.3390/ijms232415744

Butt TR, Edavettal SC, Hall JP, Mattern MR (2005) SUMO fusion technology for difficult-to-express proteins. Protein Expr Purif 43:1–9. https://doi.org/10.1016/j.pep.2005.03.016

Byambasuren O, Stehlik P, Clark J, Alcorn K, Glasziou P (2023) Effect of covid-19 vaccination on long covid: systematic review. BMJ. https://doi.org/10.1136/bmjmed-2022-000385

Cao Y, Wang J, Jian F, Xiao T et al (2022) Omicron escapes the majority of existing SARS-CoV-2 neutralizing antibodies. Nature 602:657–663. https://doi.org/10.1038/s41586-021-04385-3

Chen F, Chen Y, Wang Y, Ke Q, Cui L (2022) The COVID-19 pandemic and Alzheimer's disease: mutual risks and mechanisms. Transl Neurodegener 11:1–18. https://doi.org/10.1186/s40035-022-00316-y

Chiba T, Hagihara Y, Higurashi T, Hasegawa K et al (2003) Amyloid fibril formation in the context of full-length protein: effects of proline mutations on the amyloid fibril formation of beta2-microglobulin. J Biol Chem 278:47016–47024. https://doi.org/10.1074/jbc.M304473200

Cleveland DW, Fischer SG, Kirschner MW, Laemmli UK (1977) Peptide mapping by limited proteolysis in sodium dodecyl sulfate and analysis by gel electrophoresis. J Biol Chem 252:1102–1106. https://doi.org/10.1016/S0021-9258(19)75212-0

Dagert M, Ehrlich S (1979) Prolonged incubation in calcium chloride improves the competence of *Escherichia coli* cells. Gene 6:23–28. https://doi.org/10.1016/0378-1119(79)90082-9

Dong A, Huang P, Caughey WS (1992) Redox-dependent changes in.beta.-extended chain and turn structures of cytochrome c in water solution determined by second derivative amide I infrared spectra. Biochemistry 31:182–189. https://doi.org/10.1021/bi00116a027

Ezzat K, Pernemalm M, Pålsson S, Roberts TC et al (2019) The viral protein corona directs viral pathogenesis and amyloid aggregation. Nat Commun 10:2331. https://doi.org/10.1038/s41467-019-10192-2

Farahat RA, Abdelaal A, Umar TP, El-Sakka AA et al (2022) The emergence of SARS-CoV-2 Omicron subvariants: current situation and future trends. Infez Med 30:480–494. https://doi.org/10.53854/liim-3004-2

Fitzgerald GA, Komarov A, Kaznadzey A, Mazo I, Kireeva ML (2021) Expression of SARS-CoV-2 surface glycoprotein fragment 319–640 in *E. coli*, and its refolding and purification. Protein Expr Purif 183:105861. https://doi.org/10.1016/j.pep.2021.105861

Garbuzynskiy SO, Lobanov MY, Galzitskaya OV (2010) FoldAmyloid: a method of prediction of amyloidogenic regions from protein sequence. Bioinformatics 26:326–332. https://doi.org/10.1093/bioinformatics/btp691

Gorbalenya AE, Enjuanes L, Ziebuhr J, Snijder EJ (2006) Nidovirales: evolving the largest RNA virus genome. Virus Res 117:17–37. https://doi.org/10.1016/j.virusres.2006.01.017

Gorbalenya AE, Baker SC, Baric RS, de Groot RJ et al (2020) The species severe acute respiratory syndrome-related coronavirus: classifying 2019-nCoV and naming it SARS-CoV-2. Nat Microbiol 5:536–544. https://doi.org/10.1038/s41564-020-0695-z

Greenbaum EA, Graves CL, Mishizen-Eberz AJ, Lupoli MA et al (2005) The E46K mutation in alpha-synuclein increases amyloid fibril formation. J Biol Chem 280:7800–7807. https://doi.org/10.1074/jbc.M411638200

Grobbelaar LM, Venter C, Vlok M, Ngoepe M et al (2021) SARS-CoV-2 spike protein S1 induces fibrin (ogen) resistant to fibrinolysis: implications for microclot formation in COVID-19. Biosci Rep 41:BSR20210611. https://doi.org/10.1042/BSR20210611

Gulyaeva AA, Gorbalenya AE (2021) A nidovirus perspective on SARS-CoV-2. Biochem Biophys Res Commun 538:24–34. https://doi.org/10.1016/j.bbrc.2020.11.015

Harrison AG, Lin T, Wang P (2020) Mechanisms of SARS-CoV-2 transmission and pathogenesis. Trends Immunol 41:1100–1115. https://doi.org/10.1016/j.it.2020.10.004

Hsu JT-A, Tien C-F, Yu G-Y, Shen S et al (2021) The effects of Aβ1-42 binding to the SARS-CoV-2 spike protein S1 subunit and angiotensin-converting enzyme 2. Int J Mol Sci 22:8226. https://doi.org/10.3390/ijms22158226

Huang Y, Yang C, Xu X-f, Xu W, Liu S-w (2020) Structural and functional properties of SARS-CoV-2 spike protein: potential antivirus drug development for COVID-19. Acta Pharmacol Sin 41:1141–1149. https://doi.org/10.1038/s41401-020-0485-4

Jimenez JL, Guijarro JI, Orlova E, Zurdo J et al (1999) Cryo-electron microscopy structure of an SH3 amyloid fibril and model of the molecular packing. The EMBO J 18:815–821. https://doi.org/10.1093/emboj/18.4.815

Khurana R, Coleman C, Ionescu-Zanetti C, Carter SA et al (2005) Mechanism of thioflavin T binding to amyloid fibrils. J Struct Biol 151:229–238. https://doi.org/10.1016/j.jsb.2005.06.006

Kong J, Yu S, (2007) Fourier transform infrared spectroscopic analysis of protein secondary structures. Acta Biochim Biophys Sin 39:549–559. https://doi.org/10.1111/j.1745-7270.2007.00320.x

Kronqvist N, Rising A, Johansson J (2022) A novel approach for the production of aggregation-prone proteins using the spidroin-derived NT* tag. Insoluble proteins: methods and protocols. Springer, New York

Lee CD, Sun HC, Hu SM, Chiu CF et al (2008) An improved SUMO fusion protein system for effective production of native proteins. Protein Sci 17:1241–1248

Leung W-Y, Wu HH, Floyd L, Ponnusamy A, Chinnadurai R (2023) COVID-19 infection and vaccination and its relation to amyloidosis: what do we know currently? Vaccines 11:1139. https://doi.org/10.3390/vaccines11071139

Li W, Moore MJ, Vasilieva N, Sui J et al (2003) Angiotensin-converting enzyme 2 is a functional receptor for the SARS coronavirus. Nature 426:450–454. https://doi.org/10.1038/nature02145

Liu L, Chen T, Zhou L, Sun J et al (2022) A bacterially expressed SARS-CoV-2 receptor binding domain fused with cross-reacting material 197 a-domain elicits high level of neutralizing antibodies in mice. Front Microbiol 13:854630. https://doi.org/10.3389/fmicb.2022.854630

Malone B, Urakova N, Snijder EJ, Campbell EA (2022) Structures and functions of coronavirus replication–transcription complexes and their relevance for SARS-CoV-2 drug design. Nat Rev Mol Cell Biol 23:21–39. https://doi.org/10.1038/s41580-021-00432-z

Marblestone JG, Edavettal SC, Lim Y, Lim P et al (2006) Comparison of SUMO fusion technology with traditional gene fusion systems: enhanced expression and solubility with SUMO. Protein Sci 15:182–189. https://doi.org/10.1110/ps.051812706

Marin-Argany M, Güell-Bosch J, Blancas-Mejía LM, Villegas S, Ramirez-Alvarado M (2015) Mutations can cause light chains to be too stable or too unstable to form amyloid fibrils. Protein Sci 24:1829–1840. https://doi.org/10.1002/pro.2790

Milton NG (2023) SARS-CoV-2 amyloid, is COVID-19-exacerbated dementia an amyloid disorder in the making? Front Dement 2:1233340. https://doi.org/10.3389/frdem.2023.1233340

Nystrom S, Hammarstrom P (2022) Amyloidogenesis of SARS-CoV-2 spike protein. J Am Chem Soc 144:8945–8950. https://doi.org/10.1021/jacs.2c03925

Parums DV (2023) Editorial: a rapid global increase in COVID-19 is due to the emergence of the EG.5 (Eris) subvariant of Omicron SARS-CoV-2. Med Sci Monit 29:e942244. https://doi.org/10.12659/msm.942244

Patel R, Kaki M, Potluri VS, Kahar P, Khanna D (2022) A comprehensive review of SARS-CoV-2 vaccines: Pfizer, moderna & Johnson & Johnson. Hum Vaccin Immunother 18:2002083. https://doi.org/10.1080/21645515.2021.2002083

Sarr M, Kronqvist N, Chen G, Aleksis R et al (2018) A spidroin-derived solubility tag enables controlled aggregation of a designed amyloid protein. FEBS J 285:1873–1885. https://doi.org/10.1111/febs.14451

Shin HJ, Ku KB, Kim HS, Moon HW et al (2021) Receptor-binding domain of SARS-CoV-2 spike protein efficiently inhibits SARS-CoV-2 infection and attachment to mouse lung. Int J Biol Sci 17:3786. https://doi.org/10.7150/ijbs.61320

Starr TN, Greaney AJ, Dingens AS, Bloom JD (2021) Complete map of SARS-CoV-2 RBD mutations that escape the monoclonal antibody LY-CoV555 and its cocktail with LY-CoV016. Cell Rep Med. https://doi.org/10.1016/j.xcrm.2021.100255

Stefani M, Dobson CM (2003) Protein aggregation and aggregate toxicity: new insights into protein folding, misfolding diseases and biological evolution. J Mol Med 81:678–699. https://doi.org/10.1007/s00109-003-0464-5

Susi H, Byler DM (1986) Resolution-enhanced fourier transform infrared spectroscopy of enzymes. Methods Enzymol 130:290–311. https://doi.org/10.1016/0076-6879(86)30015-6

Tayeb-Fligelman E, Bowler JT, Tai CE, Sawaya MR et al (2023) Low complexity domains of the nucleocapsid protein of SARS-CoV-2 form amyloid fibrils. Nat Commun 14:2379. https://doi.org/10.1038/s41467-023-37865-3

WHO Coronavirus (COVID-19) Dashboard (2024) Retrieved 11 July from covid19.who.int/

Wu A, Peng Y, Huang B, Ding X et al (2020) Genome composition and divergence of the novel coronavirus (2019-nCoV) originating in China. Cell Host Microbe 27:325–328. https://doi.org/10.1016/j.chom.2020.02.001

Yang S, Li Y, Dai L, Wang J et al (2021) Safety and immunogenicity of a recombinant tandem-repeat dimeric RBD-based protein subunit vaccine (ZF2001) against

COVID-19 in adults: two randomised, double-blind, placebo-controlled, phase 1 and 2 trials. Lancet Infect Dis 21:1107–1119. https://doi.org/10.1016/S1473-3099(21)00127-4

Young LM, Mahood RA, Saunders JC, Tu L-H et al (2015) Insights into the consequences of co-polymerisation in the early stages of IAPP and Aβ peptide assembly from mass spectrometry. Analyst 140:6990–6999. https://doi.org/10.1039/C5AN00865D